Paper 5

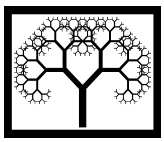

Proceedings of the Seventh International Conference
on Computational Structures Technology,
B.H.V. Topping and C.A. Mota Soares (Editors),
Civil-Comp Press, Stirling, Scotland.

Finite Element Modelling of Beams with Arbitrary Active Constrained Layer Damping Treatments

C.M.A. Vasques†, B. Mace‡, P. Gardonio‡ and J.D. Rodrigues†
† Department of Mechanical Engineering and Industrial Management
Faculty of Engineering, University of Porto, Portugal
‡ Institute of Sound and Vibration Research
University of Southampton, United Kingdom

Abstract

This paper concerns arbitrary active constrained layer damping (ACLD) treatments applied to beams. In order to suppress vibration, hybrid active-passive treatments composed of piezoelectric and viscoelastic layers are mounted on the substrate beam structure. These treatments combine the high capacity of passive viscoelastic materials to dissipate vibrational energy at high frequencies with the active capacity of piezoelectric materials at low frequencies. The aim of this research is the development of a generic analytical formulation that can describe these hybrid couplings in an accurate and consistent way. The analytical formulation considers a partial layer-wise theory, with an arbitrary number of layers, both viscoelastic and piezoelectric, attached to both surfaces of the beam. A fully coupled electro-mechanical theory for modelling the piezoelectric layers is considered. The equations of motion, electric charge equilibrium and boundary conditions are presented. A one-dimensional finite element (FE) model is developed, with the nodal degrees of freedom being the axial and transverse displacements and the rotation of the centreline of the host beam, the rotations of the individual layers and the electric potentials of each piezoelectric layer. The damping behavior of the viscoelastic layers is modeled by the complex modulus approach. Three frequency response functions were measured experimentally and evaluated numerically: acceleration per unit force, acceleration per unit voltage into the piezoelectric actuator and induced voltage per unit force. The numerical results are presented and compared with experimental results to validate the FE model.

Keywords: beam, viscoelastic, piezoelectric, active constrained layer damping, finite element.

1 Introduction

Passive damping treatments have been extensively used in engineering to reduce vibration and noise radiation. The simplest form of passive damping is the one where single layers of viscoelastic materials are attached to the host structure. When the structure vibrates energy is dissipated in the viscoelastic layer. Increasing the thickness and length of the viscoelastic treatment would increase the energy dissipation and consequently the damping. However, in applications where the weight is of critical importance, a more efficient treatment is required, and other alternatives to increase damping must be found.

It is well recognized that the inclusion of elastic constraining layers covering the viscoelastic layer can enhance the energy dissipation through an increase in shear deformations. That is known as *passive constrained layer damping* (PCLD). However, while passive damping treatments can greatly improve damping of the system, there are limitations. Viscoelastic materials have frequency and temperature dependent mechanical properties which can make the damping change, bringing limitations to the effective temperature and frequency range of the treatment. In order to provide adequate damping over a broad frequency band, different viscoelastic materials must be chosen which often complicates analysis and design of the system. Therefore, while viscoelastic treatments are easy to apply, the damping is often of limited bandwidth.

In the last decade *active constrained layer damping* (ACLD) treatments have been applied to structures. Those are hybrid treatments with constraining layers made of piezoelectric materials. One of the unique features of piezoelectric materials is that they can serve both as sensors and actuators. If utilized as actuators, and according to an appropriate control law, the active constraining layer can increase the shear deformation of the viscoelastic layer and overcome some of the PCLD limitations. The ACLD treatments combine the high capacity of passive viscoelastic materials to dissipate vibrational energy at high frequencies with the active capacity of piezoelectric materials at low frequencies. Therefore, in the same damping treatment, a broader band control is achieved benefiting from the advantages of both passive (simplicity, stability, fail-safe, low-cost) and active (adaptability, high-performance) systems.

Various configurations of active and passive layers have been proposed in an attempt to improve performance. In general so-called hybrid active-passive (or arbitrary ACLD) treatments involving arbitrary arrangements of constraining and passive layers, integrating piezoelectric sensors and actuators, might be utilized. A survey of advances in hybrid active-passive vibrations and noise control via piezoelectric and viscoelastic constrained layer treatments can be found in references [1, 2].

Modeling this kind of structural system often requires a coupled model of the structure, which comprises piezoelectric, viscoelastic and elastic layers. These treatments are applied to beams, plates and shells. They can be modeled as either lumped or distributed parameter systems, and usually have complicated geometries that make analytical solution of the equations of motion difficult, if not impossible. Alternatively, various discretization techniques, such as finite element (FE) modelling, modal analy-

sis, and lumped parameters models, allow the approximation of the partial differential equations by a finite set of ordinary differential equations.

The temperature and frequency dependent material properties of the viscoelastic materials put some difficulties on the mathematical model, increasing its complexity. Usually the temperature is assumed constant and only models concerning frequency dependence are utilized. The simplest way of modelling those materials is achieved by a *complex modulus approach* (CMA) where the material properties are assumed frequency independent. The CMA is a frequency domain method that is limited to steady state vibrations and single-frequency harmonic excitations [3]. Time domain models such as the *Golla-Hughes-McTavish* (GHM) model [4], *anelastic displacement fields* (ADF) approach [5] or *fractional calculus approach* [6], have been developed in the last few years and represent good alternatives to the CMA when the study of transient response is of interest.

In the development of FE models with piezoelectric actuators or sensors, different assumptions can be taken into account in the theoretical model when considering the electro-mechanical coupling. A survey on the advances in FE modelling of piezoelectric adaptive structures is presented by Benjeddou [7]. These assumptions regard mainly the use (or not) of electric degrees of freedom (DoF) and the approximations of the through-the-thickness variation of the electric potential. Therefore, they lead to decoupled, partial and fully coupled electro-mechanical theories, which in turn can lead to different modifications of the structure's stiffness and different approximations of the physics of the system.

When designing hybrid active-passive treatments it is important to know the configuration of the structure and treatment that gives optimal damping. For simulation the designer needs a model of the system in order to define the optimal locations, thicknesses, configurations, control law, etc. The alternatives are diverse. The aim of this work is the development of a generic analytical model that can account for the hybrid couplings in an accurate and consistent way. It can therefore be seen as an initial step from which different analytical and discretization methods can be used for the solution of arbitrary hybrid active-passive treatments on beams. We start by presenting the structural analytical model of a composite beam with an arbitrary number of layers of elastic, piezoelectric and viscoelastic materials, attached to both surfaces of the beam. The kinematic assumptions, based in a partial layerwise theory, are first presented. Then, the electric model assumptions for the piezoelectric materials which account for a fully coupled electro-mechanical theory are described. Moreover, the damping behavior of the viscoelastic layers, modeled by the CMA, is presented. Hamilton's principle is utilized to derive the equations of motion and electric charge equilibrium, and the electro-mechanical boundary conditions. The strong forms of the general analytical model of the composite beam with an arbitrary number of layers are then presented by a set of partial differential equations. A FE model solution is presented and a composite beam FE is derived from the weak forms of the analytical model. Finally, the developed FE is used in the prediction of three frequency response functions: acceleration per unit force and voltage into the piezoelectric actuator and

induced voltage per unit force. Numerical results are presented and compared with experimental results to validate the FE numerical tool.

2 Analytical Model

In this section the analytical model for a beam with arbitrary ACLD treatments is developed. For the sake of brevity some intermediate steps on the development of the equations of motion and boundary conditions are omitted. The reader is referred to the work of Vasques et al. [8] for further details.

2.1 Displacements and Strains

Consider the layered beam illustrated in Figure 1. The composite beam consists of a host beam, layer 0, of thickness $2h_0$, to which other layers (treatments) are attached. In order to be able to model several configurations of the treatments, the composite beam theory allows an arbitrary number of layers of elastic, piezoelectric and viscoelastic materials in arbitrary positions. The displacement field is defined according to a partial layerwise theory where the axial and transverse displacements, $\tilde{u}_k(x, z_k, t)$ and $\tilde{w}_k(x, t)$, of the top ($n = 1, \ldots, \bar{n}$), core ($c = 0$) and bottom ($m = \bar{m}, \ldots, -1$) layers are given by

$$\begin{aligned}
\tilde{u}_n(x, z_n, t) &= u_0(x, t) + h_0\theta_0(x, t) + \sum_{i=1}^{n-1} 2h_i\theta_i(x, t) + (z_n + h_n)\theta_n(x, t), \\
\tilde{u}_c(x, z_c, t) &= u_0(x, t) + z_0\theta_0(x, t), \\
\tilde{u}_m(x, z_m, t) &= u_0(x, t) - h_0\theta_0(x, t) - \sum_{i=m+1}^{-1} 2h_i\theta_i(x, t) + (z_m - h_m)\theta_m(x, t), \\
\tilde{w}_k(x, t) &= \tilde{w}_n(x, t) = \tilde{w}_c(x, t) = \tilde{w}_m(x, t) = w_0(x, t),
\end{aligned} \tag{1}$$

where $2h_k$ is the thickness of the k-th layer ($k = \bar{m}, \ldots, -1, 0, 1, \ldots, \bar{n}$), $u_0(x, t)$, $w_0(x, t)$ and $\theta_0(x, t)$ are, respectively, the generalized axial and transverse displacements and the rotation of the beam's mid-plane, and $\theta_n(x, t)$ and $\theta_m(x, t)$ are the rotation of each n-th top and m-th bottom layer. It is worth noting that positive indices are used to denote the top layers and negative indices are used to the bottom ones, i.e., $n > 0$ and $m < 0$. The z-coordinates in Equations (1) are measured from the interface between layers n and $n - 1$ ($z_n + h_n$) and m and $m + 1$ ($z_m - h_m$). They represent a translation of the rotation axis of each top and bottom layer from the layer mid-plane to the interface of the adjacent layer. Note that axial displacement continuity at the interfaces of the layers is assured, leading to coupling terms in the axial displacements of the layers, and that a constant through-the-thickness transverse displacement $w_0(x, t)$ is assumed.

According to the displacement field (1) the extensional and shear strains of the

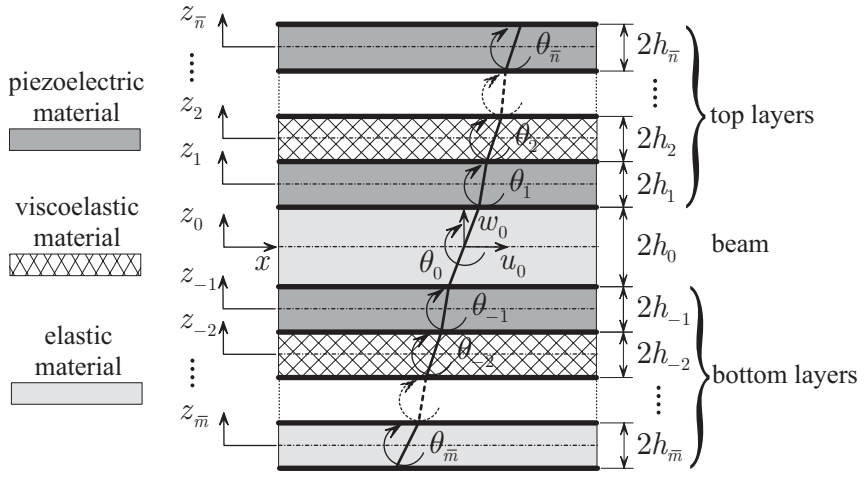

Figure 1: Layerwise displacement field of the beam with arbitrary ACLD treatments.

layers are determined by the usual linear strain-displacement relations, to be

$$
\begin{aligned}
S^n_{xx} = \frac{\partial \tilde{u}_n}{\partial x} &= u'_0 + h_0\theta'_0 + \sum_{i=1}^{n-1} 2h_i\theta'_i + (z_n + h_n)\theta'_n, \\
S^c_{xx} = \frac{\partial \tilde{u}_c}{\partial x} &= u'_0 + z_0\theta'_0, \\
S^m_{xx} = \frac{\partial \tilde{u}_m}{\partial x} &= u'_0 - h_0\theta'_0 - \sum_{i=m+1}^{-1} 2h_i\theta'_i + (z_m - h_m)\theta'_m, \\
S^k_{xz} = \frac{\partial \tilde{w}_k}{\partial x} - \frac{\partial \tilde{u}_k}{\partial z_k} &= w'_0 - \theta_k,
\end{aligned}
\tag{2}
$$

where the notation $(\cdot)'$ is used to denote the spatial derivative in the x-direction. Note that the kinematic hypotheses considered previously lead to null transverse strains and a first-order shear deformation theory (FSDT) for all the layers.

2.2 Constitutive Equations

Consider a general piezoelectric layer. The material of the piezoelectric layers is assumed to be orthotropic with the axes of orthotropy parallel to the axes of the beam. These materials are polarized in the transverse direction and have the behavior of normal piezoelectric materials, with the symmetry properties of an orthorhombic crystal of the class $mm2$ [9]. The linear piezoelectric constitutive equations are

$$
\mathbf{T} = \mathbf{c}^E\mathbf{S} - \mathbf{e}^{\mathrm{T}}\mathbf{E}, \;\; \mathbf{D} = \mathbf{e}\mathbf{S} + \boldsymbol{\varepsilon}^S\mathbf{E}, \tag{3a,b}
$$

where $\mathbf{T}$, $\mathbf{S}$, $\mathbf{E}$ and $\mathbf{D}$ are, respectively, the stress, strain, electric field and electric displacement vectors, and $\mathbf{c}^E$, $\mathbf{e}^{\mathrm{T}}$ and $\boldsymbol{\varepsilon}^S$ are, respectively, the elasticity (at constant electric field), transpose piezoelectric and dielectric (at constant strain) matrices appropriate for the material.

The displacement field considered in (1) is independent of the y-axis and null along that direction. Hence the constitutive equations of a generic top or bottom piezoelectric layer p can be written in the following reduced form,

$$\begin{Bmatrix} T_{xx}^p \\ T_{xz}^p \end{Bmatrix} = \begin{bmatrix} c_{11}^{*p} & 0 \\ 0 & c_{55}^p \end{bmatrix} \begin{Bmatrix} S_{xx}^p \\ S_{xz}^p \end{Bmatrix} - \begin{bmatrix} 0 & e_{31}^{*p} \\ e_{15}^p & 0 \end{bmatrix} \begin{Bmatrix} E_x^p \\ E_z^p \end{Bmatrix}, \tag{4a}$$

$$\begin{Bmatrix} D_x^p \\ D_z^p \end{Bmatrix} = \begin{bmatrix} 0 & e_{15}^p \\ e_{31}^{*p} & 0 \end{bmatrix} \begin{Bmatrix} S_{xx}^p \\ S_{xz}^p \end{Bmatrix} + \begin{bmatrix} \varepsilon_{11}^p & 0 \\ 0 & \varepsilon_{33}^{*p} \end{bmatrix} \begin{Bmatrix} E_x^p \\ E_z^p \end{Bmatrix}, \tag{4b}$$

with

$$c_{11}^{*p} = c_{11}^p - \frac{{c_{13}^p}^2}{c_{33}^p},\ e_{31}^{*p} = e_{31}^p - e_{33}^p \frac{c_{13}^p}{c_{33}^p},\ \varepsilon_{33}^{*p} = \varepsilon_{33}^p + \frac{{e_{33}^p}^2}{c_{33}^p}. \tag{5a-c}$$

The modification of constants c_{11}^p, e_{31}^p and ε_{33}^p is due to the transverse stress assumption, $T_{zz}^p \approx 0$. Furthermore, for the characterization of the core layer or any other viscoelastic or elastic layer, Equation (4a) can also be used by setting the piezoelectric contants e_{31}^{*p} and e_{15}^p to zero and by using the appropriate values for the elasticity matrix.

2.3 Piezoelectric Materials Model

In the present work, a fully coupled electromechanical theory which takes into account the direct piezoelectric effect with a non-linear distribution of the electric potential is utilized. The electric displacement vector in Equation (4b) can be written as

$$\begin{Bmatrix} D_x^p \\ D_z^p \end{Bmatrix} = \begin{bmatrix} \varepsilon_{11}^p & 0 \\ 0 & \varepsilon_{33}^{*p} \end{bmatrix} \begin{Bmatrix} E_x^p - \bar{E}_x^p \\ E_z^p - \bar{E}_z^p \end{Bmatrix}, \text{ with } \bar{E}_x^p = -\frac{e_{15}^p}{\varepsilon_{11}^p} S_{xz}^p,\ \bar{E}_z^p = -\frac{e_{31}^{*p}}{\varepsilon_{33}^{*p}} S_{xx}^p, \tag{6}$$

where $\bar{E}_x^p$ and $\bar{E}_z^p$ are the electric fields induced by the mechanical strains.

According to reference [10], for electroded layers with the electric potential being prescribed and with the assumption of zero electric displacement in the x-direction, the axial and transverse electric fields, E_x^p and E_z^p, and the electric potential φ_p are given by

$$E_x^p = \bar{E}_x^p,\ E_z^p = -\frac{\phi_p}{2h_p} + \bar{E}_z^p - \frac{1}{2h_p}\int_{-h_p}^{h_p} \bar{E}_z^p \mathrm{d}z_p, \tag{7a,b}$$

$$\varphi_p = \frac{\phi_p}{2h_p}(z_p + h_p) - \int_{-h_p}^{z_p} \bar{E}_z^p \mathrm{d}z_p + \frac{(z_p + h_p)}{2h_p}\int_{-h_p}^{h_p} \bar{E}_z^p \mathrm{d}z_p, \tag{8}$$

where ϕ_p denotes the electrical potential difference of the electrodes at each piezoelectric layer. Substituting into Equations (7) and (8) the induced electric fields in (6) and considering the strain definitions in (2), the electric field and potential become [11]

$$E_x^p = -\frac{e_{15}^p}{\varepsilon_{11}^p}\left(w_0' - \theta_p\right),\ E_z^p = -\frac{\phi_p}{2h_p} - \frac{e_{31}^{*p}}{\varepsilon_{33}^{*p}} z_p \theta_p', \tag{9a,b}$$

$$\varphi_p = \frac{\phi_p}{2h_p}\left(z_p + h_p\right) + \frac{1}{2}\frac{e_{31}^{*p}}{\varepsilon_{33}^{*p}}\left({z_p}^2 - {h_p}^2\right)\theta_p'. \tag{10}$$

It is worth noting that the first part of Equation (10) is a linear through-the-thickness electric potential term concerning the applied electric potential difference and the second part is a parabolic term concerning the induced potential due to the mechanical strains.

2.4 Viscoelastic Materials Model

Viscoelastic materials are a class of materials which exhibit a strong temperature and frequency dependent constitutive behavior. They can be characterized in the frequency domain by a complex shear or extensional modulus, $G(\omega)$ or $E(\omega)$, and a loss factor $\eta(\omega)$ which accounts for energy dissipation effects. Considering simple harmonic excitation and a fixed temperature, it is possible to use the CMA to describe the viscoelastic behavior, by putting

$$G(\omega) = G'(\omega) + jG''(\omega), \tag{11}$$

where $G'(\omega)$ is the shear storage modulus, $G''(\omega)$ is the shear loss modulus, ω is the frequency and $j = \sqrt{-1}$. Defining Equation (11) in terms of the loss factor yields

$$G(\omega) = G'(\omega)[1 + j\eta(\omega)], \ \eta(\omega) = \frac{G''(\omega)}{G'(\omega)}. \tag{12a,b}$$

If we consider a linear, homogeneous and isotropic viscoelastic material, the Young storage modulus $E'(\omega)$ and shear storage modulus $G'(\omega)$ are related by

$$G'(\omega) = \frac{E'(\omega)}{2[1 + \nu(\omega)]}, \tag{13}$$

where $\nu(\omega)$ is the Poisson's ratio. In general, the complex moduli $E(\omega)$ and $G(\omega)$ are not proportional because the Poisson's ratio is also frequency dependent and the loss factors $\eta_E(\omega)$ and $\eta_G(\omega)$ are not equal. However, for simplicity one can relax that condition and put $\eta_E(\omega) = \eta_G(\omega) = \eta(\omega)$.

2.5 Variational Formulation

In order to derive the electromechanical equations of motion and boundary conditions of the composite beam with ACLD treatments, Hamilton's principle is used, where the Lagrangian and the applied forces work are adapted for the electrical and mechanical contributions [12], so that

$$\int_{t_0}^{t_1} (\delta T - \delta H + \delta W)\, \mathrm{d}t = 0, \tag{14}$$

where t_0 and t_1 define the time interval, T is the kinetic energy, H is the electromechanical enthalpy (energy stored in the piezoelectric and non-piezoelectric layers) and W denotes the work done by the applied mechanical forces and electrical charges. In the following, it will be assumed that all the top and bottom layers are piezoelectric. However, the formulation still holds for non piezoelectric layers by considering only the mechanical virtual work terms for those layers.

2.5.1 Virtual Work of the Internal Electromechanical Forces

The work of the internal electromechanical forces is given by the sum of the virtual work contributions of all the layers. Considering a generic piezoelectric layer $p = n, m = \bar{m}, \ldots, -1, 1, \ldots, \bar{n}$, and separating the total virtual work δH^p into mechanical δH^p_{uu}, piezoelectric $\delta H^p_{u\phi}$ and $\delta H^p_{\phi u}$, and dielectric $\delta H^p_{\phi\phi}$ terms, for the piezoelectric layers of volume V_p, yields

$$\delta H^p = \delta H^p_{uu} - \delta H^p_{u\phi} - \delta H^p_{\phi u} - \delta H^p_{\phi\phi}, \tag{15}$$

where

$$\delta H^p_{uu} = \int_{V_p} (\delta S^p_{xx} c^{*p}_{11} S^p_{xx} + \delta S^p_{xz} c^p_{55} S^p_{xz})\, \mathrm{d}V_p, \tag{16}$$

$$\delta H^p_{u\phi} = \int_{V_p} (\delta S^p_{xx} e^{*p}_{31} E^p_z + \delta S^p_{xz} e^p_{15} E^p_x) \mathrm{d}V_p, \tag{17}$$

$$\delta H^p_{\phi u} = \int_{V_p} (\delta E^p_z e^{*p}_{31} S^p_{xx} + \delta E^p_x e^p_{15} S^p_{xz}) \mathrm{d}V_p, \tag{18}$$

$$\delta H^p_{\phi\phi} = \int_{V_p} (\delta E^p_x \varepsilon^p_{11} E^p_x + \delta E^p_z \varepsilon^{*p}_{33} E^p_z) \mathrm{d}V_p. \tag{19}$$

As can be seen in Equation (10) the electric field definitions are expressed in terms of the electric potential difference and mechanical strains. Thus, Equations (17)-(19) can be partitioned in the electro-mechanical terms, $\delta H^{p(\phi)}_{u\phi}$, $\delta H^{p(\phi)}_{\phi u}$ and $\delta H^{p(\phi)}_{\phi\phi}$, expressed in terms of the electrical potential difference and mechanical strains, and in the induced terms $\delta \bar{H}^{p(\phi)}_{u\phi}$, $\delta \bar{H}^{p(\phi)}_{\phi u}$ and $\delta \bar{H}^{p(\phi)}_{\phi\phi}$, which are expressed only in terms of the bending and shear mechanical strains, yielding

$$\delta H^p_{u\phi} = -\delta H^{p(\phi)}_{u\phi} - \delta \bar{H}^{p(\phi)}_{u\phi}, \;\; \delta H^p_{\phi u} = -\delta H^{p(\phi)}_{\phi u} - \delta \bar{H}^{p(\phi)}_{\phi u}, \tag{20a,b}$$

$$\delta H^p_{\phi\phi} = \delta H^{p(\phi)}_{\phi\phi} + \delta \bar{H}^{p(\phi)}_{\phi\phi}. \tag{21}$$

Therefore, the electro-mechanical terms expressed only in terms of the strains can be summed with the pure mechanical ones, δH^p_{uu}, yielding

$$\delta H^{p(\phi)}_{uu} = \delta H^p_{uu} + \delta \bar{H}^{p(\phi)}_{u\phi} + \delta \bar{H}^{p(\phi)}_{\phi u} - \delta \bar{H}^{p(\phi)}_{\phi\phi}, \tag{22}$$

and Equation (15) becomes

$$\delta H^p = \delta H^{p(\phi)}_{uu} + \delta H^{p(\phi)}_{u\phi} + \delta H^{p(\phi)}_{\phi u} + \delta H^{p(\phi)}_{\phi\phi}. \tag{23}$$

Expression (22) represents the stiffness increase due to the direct piezoelectric effect where the effects of the axial and transverse induced electric fields are condensed in Equation (16). See [8] for further details.

Considering in Equation (23) the strain definitions (2) and the first part of the transverse electric field in Equation (9b) and integrating by parts, we have for the core, top and bottom layers,

$$\delta H^c_{uu} = \delta \hat{H}^c_{uu} - \delta \tilde{H}^c_{uu}, \tag{24}$$

$$\delta H_{uu}^{n(\phi)} = \delta \hat{H}_{uu}^{n(\phi)} - \delta \tilde{H}_{uu}^{n(\phi)},\ \delta H_{uu}^{m(\phi)} = \delta \hat{H}_{uu}^{m(\phi)} - \delta \tilde{H}_{uu}^{m(\phi)}, \tag{25a,b}$$

where

$$\delta \hat{H}_{uu}^{c} = \Big[\delta u_0 c_{11}^{*c} A_c u_0' + \delta w_0 \left(c_{55}^{c} A_c w_0' - c_{55}^{c} A_c \theta_0\right) + \delta \theta_0 c_{11}^{*c} I_c \theta_0'\Big]_0^L, \tag{26}$$

$$\begin{aligned}\delta \tilde{H}_{uu}^{c} = \int_L \Big[&\delta u_0 c_{11}^{*c} A_c u_0'' + \delta w_0 \left(c_{55}^{c} A_c w_0'' - c_{55}^{c} A_c \theta_0'\right) \\ &+ \delta \theta_0 \left(c_{11}^{*c} I_c \theta_0'' + c_{55}^{c} A_c w_0' - c_{55}^{c} A_c \theta_0\right)\Big] \mathrm{d}L\end{aligned} \tag{27}$$

and

$$\begin{aligned}\delta \hat{H}_{uu}^{n(\phi)} = \Big[&\delta u_0 \Big(c_{11}^{*n} A_n u_0' + c_{11}^{*n} h_0 A_n \theta_0' + c_{11}^{*n} \sum_{i=1}^{n-1} 2h_i A_n \theta_i' + c_{11}^{*n} \bar{I}_n \theta_n'\Big) \\ &+ \delta w_0 \Big(\bar{c}_{55}^{n(\phi)} A_n w_0' - \bar{c}_{55}^{n(\phi)} A_n \theta_n\Big) + \delta \theta_0 \Big(c_{11}^{*n} h_0 A_n u_0' + c_{11}^{*n} {h_0}^2 A_n \theta_0' \\ &+ c_{11}^{*n} h_0 \sum_{i=1}^{n-1} 2h_i A_n \theta_i' + c_{11}^{*n} h_0 \bar{I}_n \theta_n'\Big) + \sum_{i=1}^{n-1} \delta \theta_i \Big(c_{11}^{*n} 2h_i A_n u_0' + c_{11}^{*n} 2h_i h_0 A_n \theta_0' \\ &+ c_{11}^{*n} 4h_i \sum_{j=1}^{n-1} h_j A_n \theta_j' + c_{11}^{*n} 2h_i \bar{I}_n \theta_n'\Big) + \delta \theta_n \Big(c_{11}^{*n} \bar{I}_n u_0' + c_{11}^{*n} h_0 \bar{I}_n \theta_0' \\ &+ c_{11}^{*n} \sum_{i=1}^{n-1} 2h_i \bar{I}_n \theta_i' + \bar{c}_{11}^{n(\phi)} I_n \theta_n'\Big)\Big]_0^L,\end{aligned} \tag{28}$$

$$\begin{aligned}\delta \tilde{H}_{uu}^{n(\phi)} = \int_L \Big[&\delta u_0 \Big(c_{11}^{*n} A_n u_0'' + c_{11}^{*n} h_0 A_n \theta_0'' + c_{11}^{*n} \sum_{i=1}^{n-1} 2h_i A_n \theta_i'' + c_{11}^{*n} \bar{I}_n \theta_n''\Big) \\ &+ \delta w_0 \Big(\bar{c}_{55}^{n(\phi)} A_n w_0'' - \bar{c}_{55}^{n(\phi)} A_n \theta_n'\Big) + \delta \theta_0 \Big(c_{11}^{*n} h_0 A_n u_0'' + c_{11}^{*n} {h_0}^2 A_n \theta_0'' \\ &+ c_{11}^{*n} h_0 \sum_{i=1}^{n-1} 2h_i A_n \theta_i'' + c_{11}^{*n} h_0 \bar{I}_n \theta_n''\Big) + \sum_{i=1}^{n-1} \delta \theta_i \Big(c_{11}^{*n} 2h_i A_n u_0'' + c_{11}^{*n} 2h_i h_0 A_n \theta_0'' \\ &+ c_{11}^{*n} 4h_i \sum_{j=1}^{n-1} h_j A_n \theta_j'' + c_{11}^{*n} 2h_i \bar{I}_n \theta_n''\Big) + \delta \theta_n \Big(c_{11}^{*n} \bar{I}_n u_0'' + c_{11}^{*n} h_0 \bar{I}_n \theta_0'' \\ &+ c_{11}^{*n} \sum_{i=1}^{n-1} 2h_i \bar{I}_n \theta_i'' + \bar{c}_{11}^{n(\phi)} I_n \theta_n'' + \bar{c}_{55}^{n(\phi)} A_n w_0' - \bar{c}_{55}^{n(\phi)} A_n \theta_n\Big)\Big] \mathrm{d}L.\end{aligned} \tag{29}$$

Similar expressions to (28) and (29) can be found for the bottom layers, cf. [8]. Furthermore, integrating the electrical terms in Equation (23) by parts yields

$$\delta H_{u\phi}^{n(\phi)} = \delta \hat{H}_{u\phi}^{n(\phi)} - \delta \tilde{H}_{u\phi}^{n(\phi)},\ \delta H_{u\phi}^{m(\phi)} = \delta \hat{H}_{u\phi}^{m(\phi)} - \delta \tilde{H}_{u\phi}^{m(\phi)}, \tag{30a,b}$$

where

$$\delta \hat{H}_{u\phi}^{n(\phi)} = \Big[\frac{e_{31}^{*n}}{2h_n} \phi_n \Big(A_n \delta u_0 + h_0 A_n \delta \theta_0 + \sum_{i=1}^{n-1} 2h_i A_n \delta \theta_i + \bar{I}_n \delta \theta_n\Big)\Big]_0^L, \tag{31}$$

$$\delta \tilde{H}_{u\phi}^{n(\phi)} = \int_L \frac{e_{31}^{*n}}{2h_n} \phi_n' \Big(A_n \delta u_0 + h_0 A_n \delta \theta_0 + \sum_{i=1}^{n-1} 2h_i A_n \delta \theta_i + \bar{I}_n \delta \theta_n\Big) \mathrm{d}L. \tag{32}$$

Again, similar expressions to (31) and (32) can be found for the bottom layers.

In the previous equations integration with respect to z_k across the layer was carried out where L is the length of the beam and A_k, $\bar{I}_p$ and I_k represent the zero, first and second order moments of area, respectively. They are given by

$$A_k = 2h_k b,\ \bar{I}_n = \frac{(2h_n)^2 b}{2},\ \bar{I}_m = -\frac{(2h_m)^2 b}{2},\ I_p = \frac{(2h_p)^3 b}{3},\ I_c = \frac{(2h_c)^3 b}{12}, \quad \text{(33a-e)}$$

where b is the width of the beam. The stiffness increase due to the induced electric fields expressed in Equation (22) is represented by the so-called effective stiffness parameters [11],

$$\bar{c}_{11}^{p(\phi)} = c_{11}^{*p} + \frac{e_{31}^{*p\ 2}}{4\bar{\varepsilon}_{33}^{*p}},\ \bar{c}_{55}^{p(\phi)} = c_{55}^{p} + \frac{e_{15}^{p\ 2}}{\bar{\varepsilon}_{11}^{p}}. \quad \text{(34a,b)}$$

As can be seen in (28) and (29), the parameter $\bar{c}_{11}^{p(\phi)}$ only affects the bending stiffness and it represents the effects of the induced parabolic electric potential. Regarding $\bar{c}_{55}^{p(\phi)}$, it represents the stiffness increase due to the assumption that the x-component of the electric displacement vector vanishes and it affects only the shear stiffness.

Finally, the total virtual work of the internal electromechanical forces in all the layers (elastic, piezoelectric or viscoelastic layers) is given by

$$\delta H = \delta H_{uu}^{c} + \sum_{\substack{p=\bar{m} \\ p\neq 0}}^{\bar{n}} \Big(\delta H_{uu}^{p(\phi)} + \delta H_{u\phi}^{p(\phi)} + \delta H_{\phi u}^{p(\phi)} - \delta H_{\phi\phi}^{p(\phi)} \Big). \quad \text{(35)}$$

2.5.2 Virtual Work of the Inertial Forces

The virtual work of the inertial forces in a generic layer k is given by

$$\delta T^k = -\int_{V_k} \rho_k \Big(\delta\tilde{u}_k \ddot{\tilde{u}}_k + \delta\tilde{w}_k \ddot{\tilde{w}}_k \Big) \mathrm{d}V_k, \quad \text{(36)}$$

where ρ_k is the density of the material into layer. Substituting the displacement field in Equation (1) into (36) gives, after integration, for the core and generic top layers,

$$\begin{aligned}
\delta T^n = -\int_L \Big[& \delta u_0 \Big(\rho_n A_n \ddot{u}_0 + \rho_n h_0 A_n \ddot{\theta}_0 + \rho_n \sum_{i=1}^{n-1} 2h_i A_n \ddot{\theta}_i + \rho_n \bar{I}_n \ddot{\theta}_n \Big) \\
& - \delta\theta_0 \Big(\rho_n h_0 A_n \ddot{u}_0 + \rho_n {h_0}^2 A_n \ddot{\theta}_0 + \rho_n h_0 \sum_{i=1}^{n-1} 2h_i A_n \ddot{\theta}_i + \rho_n h_0 \bar{I}_n \ddot{\theta}_n \Big) \\
& - \sum_{i=1}^{n-1} \delta\theta_i \Big(\rho_n 2h_i A_n \ddot{u}_0 + \rho_n 2h_i h_0 A_n \ddot{\theta}_0 + \rho_n 4h_i \sum_{j=1}^{n-1} h_j A_n \ddot{\theta}_j + \rho_n 2h_i \bar{I}_n \ddot{\theta}_n \Big) \\
& - \delta\theta_n \Big(\rho_n \bar{I}_n \ddot{u}_0 + \rho_n h_0 \bar{I}_n \ddot{\theta}_0 + \rho_n \sum_{i=1}^{n-1} 2h_i \bar{I}_n \ddot{\theta}_i + \rho_n I_n \ddot{\theta}_n \Big) - \delta w_0 \rho_n A_n \ddot{w}_0 \Big] \mathrm{d}L,
\end{aligned} \quad \text{(37)}$$

$$\delta T^c = -\int_L \Big(\delta u_0 \rho_c A_c \ddot{u}_0 + \delta\theta_0 \rho_c I_c \ddot{\theta}_0 + \delta w_0 \rho_c A_c \ddot{w}_0\Big) \mathrm{d}L. \tag{38}$$

As before, a similar expression to Equation (37) is obtained for the bottom layers.

The total virtual work of the inertial forces is then given by the sum of the virtual work of all the layers, i.e.,

$$\delta T = \delta T^c + \sum_{n=1}^{\bar{n}} \delta T^n + \sum_{m=\bar{m}}^{-1} \delta T^m = \sum_{k=\bar{m}}^{\bar{n}} \delta T^k. \tag{39}$$

2.5.3 Virtual Work of the External Forces

In the determination of the virtual work of the mechanical external forces, two types of applied mechanical forces are considered, namely, axial F_x^k and transverse F_z^k volume forces. The virtual work of those forces for the generic layer k is given by

$$\delta W_u^k = \int_{V_k} \Big(F_x^k \delta\tilde{u}_k + F_z^k \delta\tilde{w}_k\Big) \mathrm{d}V_k. \tag{40}$$

Substituting the displacement field (1) in (40) and integrating, yields

$$\delta W_u^n = \int_L \Big[\Big(\delta u_0 + h_0\delta\theta_0 + \sum_{i=1}^{n-1} 2h_i\delta\theta_i + h_n\delta\theta_n\Big) X_n + \delta\theta_n M_n + \delta w_0 Z_n\Big] \mathrm{d}L, \tag{41}$$

$$\delta W_u^c = \int_L \Big(\delta u_0 X_c + \delta\theta_0 M_c + \delta w_0 Z_c\Big) \mathrm{d}L, \tag{42}$$

where

$$\Big(X_k, M_k, Z_k\Big) = \int_{A_k} \Big(F_x^k, z_k F_x^k, F_z^k\Big) \mathrm{d}A_k. \tag{43}$$

Similar expressions to (41) can be found for the bottom layers. Thus, the total virtual work accomplished by the mechanical forces is given by

$$\delta W_u = \delta W_u^c + \sum_{n=1}^{\bar{n}} \delta W_u^n + \sum_{m=\bar{m}}^{-1} \delta W_u^n = \sum_{k=\bar{m}}^{\bar{n}} \delta W_u^k. \tag{44}$$

The virtual work of the electric charge density in a generic piezoelectric layer is defined by

$$\delta W_\phi^p = -\int_{A_p^e} \delta\varphi_p \tau_p \mathrm{d}A_p^e = -\int_L \delta\phi_p b \tau_p \mathrm{d}L, \tag{45}$$

where A_p^e is the electrode area and τ_p is the applied electric charge density at the electrode. Note that from the definition of the electric potential (10), and considering only the applied potential term, one finds that $\varphi_p\left(z_p = -h_p\right) = 0$ and $\varphi_p\left(z_p = h_p\right) = \phi_p$. The total virtual work of the applied electric charge density is given by

$$\delta W_\phi = \sum_{n=1}^{\bar{n}} \delta W_\phi^n + \sum_{m=\bar{m}}^{-1} \delta W_\phi^n = \sum_{\substack{p=\bar{m} \\ p\neq 0}}^{\bar{n}} \delta W_\phi^p. \tag{46}$$

Finally, the total virtual work δW of the applied external forces, comprising the virtual work of the applied mechanical forces δW_u and that of the applied electric charge density at the electrodes δW_ϕ, is given by

$$\delta W = \delta W_u + \delta W_\phi = \sum_{k=\bar{m}}^{\bar{n}} \delta W_u^k + \sum_{\substack{p=\bar{m} \\ p\neq 0}}^{\bar{n}} \delta W_\phi^p. \tag{47}$$

2.5.4 Strong Forms

The equations of motion are obtained from the Hamilton's principle by substituting expressions (35), (39) and (47) into (14), integrating by parts and collecting the terms involving the variations δu_0, δw_0, $\delta\theta_0$, $\delta\theta_{\hat{n}}$ ($\hat{n} = 1, \ldots, \bar{n}-1$), $\delta\theta_{\bar{n}}$, $\delta\theta_{\bar{m}}$ and $\delta\theta_{\hat{m}}$ ($\hat{m} = \bar{m}+1, \ldots, -1$), independent and arbitrary in the interval $[0, L]$. The resultant equations have no solution other than the trivial one, and the differential equations of motion, with the total number of piezoelectric layers given by $\bar{p} = \bar{n} - \bar{m}$ and the total number of generalized displacements equal to $\bar{k} - 1$, with $\bar{k} = \bar{p} + 4$, are given by the following:

δu_0 :

$$\begin{aligned} &Y_{(1,1)}u_0'' + Y_{(1,3)}\theta_0'' + \sum_{\hat{n}=1}^{\bar{n}-1} Y_{(1,\hat{n}+3)}\theta_{\hat{n}}'' + Y_{(1,\bar{n}+3)}\theta_{\bar{n}}'' + Y_{(1,\bar{n}+4)}\theta_{\bar{m}}'' \\ &+ \sum_{\hat{m}=\bar{m}+1}^{-1} Y_{(1,\bar{k}+\hat{m})}\theta_{\hat{m}}'' + \sum_{n=1}^{\bar{n}} P_{(n,1)}\phi_n' + \sum_{m=\bar{m}}^{-1} P_{(\bar{p}+1+m,1)}\phi_m' + F_{(1)} = J_{(1,1)}\ddot{u}_0 \\ &+ J_{(1,3)}\ddot{\theta}_0 + \sum_{\hat{n}=1}^{\bar{n}-1} J_{(1,\hat{n}+3)}\ddot{\theta}_{\hat{n}} + J_{(1,\bar{n}+3)}\ddot{\theta}_{\bar{n}} + J_{(1,\bar{n}+4)}\ddot{\theta}_{\bar{m}} + \sum_{\hat{m}=\bar{m}+1}^{-1} J_{(1,\bar{k}+\hat{m})}\ddot{\theta}_{\hat{m}}, \end{aligned} \tag{48}$$

δw_0 :

$$\begin{aligned} &G_{(2,2)}w_0'' + G_{(2,3)}\theta_0' + \sum_{\hat{n}=1}^{\bar{n}-1} G_{(2,\hat{n}+3)}\theta_{\hat{n}}' + G_{(2,\bar{n}+3)}\theta_{\bar{n}}' + G_{(2,\bar{n}+4)}\theta_{\bar{m}}' \\ &+ \sum_{\hat{m}=\bar{m}+1}^{-1} G_{(2,\bar{k}+\hat{m})}\theta_{\hat{m}}' + F_{(2)} = J_{(2,2)}\ddot{w}_0, \end{aligned} \tag{49}$$

$\delta\theta_0$:

$$\begin{aligned} &Y_{(3,1)}u_0'' + Y_{(3,3)}\theta_0'' + \sum_{\hat{n}=1}^{\bar{n}-1} Y_{(3,\hat{n}+3)}\theta_{\hat{n}}'' + Y_{(3,\bar{n}+3)}\theta_{\bar{n}}'' + Y_{(3,\bar{n}+4)}\theta_{\bar{m}}'' + \sum_{\hat{m}=\bar{m}+1}^{-1} Y_{(3,\bar{k}+\hat{m})}\theta_{\hat{m}}'' \\ &- G_{(3,2)}w_0' - G_{(3,3)}\theta_0 + \sum_{n=1}^{\bar{n}} P_{(n,3)}\phi_n' + \sum_{m=\bar{m}}^{-1} P_{(\bar{p}+1+m,3)}\phi_m' + F_{(3)} = J_{(3,1)}\ddot{u}_0 \\ &+ J_{(3,3)}\ddot{\theta}_0 + \sum_{\hat{n}=1}^{\bar{n}-1} J_{(3,\hat{n}+3)}\ddot{\theta}_{\hat{n}} + J_{(3,\bar{n}+3)}\ddot{\theta}_{\bar{n}} + J_{(3,\bar{n}+4)}\ddot{\theta}_{\bar{m}} + \sum_{\hat{m}=\bar{m}+1}^{-1} J_{(3,\bar{k}+\hat{m})}\ddot{\theta}_{\hat{m}}, \end{aligned} \tag{50}$$

$\delta\theta_{\hat{n}}$:

$$Y_{(\hat{n}+3,1)}u_0'' + Y_{(\hat{n}+3,3)}\theta_0'' + \sum_{i=1}^{\hat{n}-1} Y_{(\hat{n}+3,i+3)}\theta_i'' + Y_{(\hat{n}+3,\hat{n}+3)}\theta_{\hat{n}}'' + \sum_{j=\hat{n}+1}^{\bar{n}-1} Y_{(\hat{n}+3,j+3)}\theta_j''$$
$$+Y_{(\hat{n}+3,\bar{n}+3)}\theta_{\bar{n}}'' - G_{(\hat{n}+3,2)}w_0' - G_{(\hat{n}+3,\hat{n}+3)}\theta_{\hat{n}} + P_{(\hat{n},\hat{n}+3)}\phi_{\hat{n}}' + \sum_{i=\hat{n}+1}^{\bar{n}} P_{(i,\hat{n}+3)}\phi_i'$$
$$+F_{(\hat{n}+3)} = J_{(\hat{n}+3,1)}\ddot{u}_0 + J_{(\hat{n}+3,3)}\ddot{\theta}_0 + \sum_{i=1}^{\hat{n}-1} J_{(\hat{n}+3,i+3)}\ddot{\theta}_i + J_{(\hat{n}+3,\hat{n}+3)}\ddot{\theta}_{\hat{n}}$$
$$+ \sum_{j=\hat{n}+1}^{\bar{n}-1} J_{(\hat{n}+3,j+3)}\ddot{\theta}_j + J_{(\hat{n}+3,\bar{n}+3)}\ddot{\theta}_{\bar{n}}, \tag{51}$$

$\delta\theta_{\bar{n}}$:

$$Y_{(\bar{n}+3,1)}u_0'' + Y_{(\bar{n}+3,3)}\theta_0'' + \sum_{\hat{n}=1}^{\bar{n}-1} Y_{(\bar{n}+3,\hat{n}+3)}\theta_{\hat{n}}'' + Y_{(\bar{n}+3,\bar{n}+3)}\theta_{\bar{n}}'' - G_{(\bar{n}+3,2)}w_0'$$
$$-G_{(\bar{n}+3,\bar{n}+3)}\theta_{\bar{n}} + P_{(\bar{n},\bar{n}+3)}\phi_{\bar{n}}' + F_{(\bar{n}+3)} = J_{(\bar{n}+3,1)}\ddot{u}_0 + J_{(\bar{n}+3,3)}\ddot{\theta}_0$$
$$+ \sum_{\hat{n}=1}^{\bar{n}-1} J_{(\bar{n}+3,\hat{n}+3)}\ddot{\theta}_{\hat{n}} + J_{(\bar{n}+3,\bar{n}+3)}\ddot{\theta}_{\bar{n}}, \tag{52}$$

$\delta\theta_{\bar{m}}$:

$$Y_{(\bar{n}+4,1)}u_0'' + Y_{(\bar{n}+4,3)}\theta_0'' + Y_{(\bar{n}+4,\bar{n}+4)}\theta_{\bar{m}}'' + \sum_{\hat{m}=\bar{m}+1}^{-1} Y_{(\bar{n}+4,\bar{k}+\hat{m})}\theta_{\hat{m}}'' - G_{(\bar{n}+4,2)}w_0'$$
$$-G_{(\bar{n}+4,\bar{n}+4)}\theta_{\bar{m}} + P_{(\bar{p}+1+\bar{m},\bar{k}+\bar{m})}\phi_{\bar{m}}' + F_{(\bar{n}+4)} = J_{(\bar{n}+4,1)}\ddot{u}_0 + J_{(\bar{n}+4,3)}\ddot{\theta}_0$$
$$+J_{(\bar{n}+4,\bar{n}+4)}\ddot{\theta}_{\bar{m}} + \sum_{\hat{m}=\bar{m}+1}^{-1} J_{(\bar{n}+4,\bar{k}+\hat{m})}\ddot{\theta}_{\hat{m}}, \tag{53}$$

$\delta\theta_{\hat{m}}$:

$$Y_{(\bar{k}+\hat{m},1)}u_0'' + Y_{(\bar{k}+\hat{m},3)}\theta_0'' + Y_{(\bar{k}+\hat{m},\bar{n}+4)}\theta_{\bar{m}}'' + \sum_{j=\bar{m}+1}^{\hat{m}-1} Y_{(\bar{k}+\hat{m},\bar{k}+j)}\theta_j'' + Y_{(\bar{k}+\hat{m},\bar{k}+\hat{m})}\theta_{\hat{m}}''$$
$$+ \sum_{i=\hat{m}+1}^{-1} Y_{(\bar{k}+\hat{m},\bar{k}+i)}\theta_i'' - G_{(\bar{k}+\hat{m},2)}w_0' - G_{(\bar{k}+\hat{m},\bar{k}+\hat{m})}\theta_{\hat{m}} + \sum_{i=\bar{m}}^{\hat{m}-1} P_{(\bar{p}+1+i,\bar{k}+\hat{m})}\phi_i'$$
$$+P_{(\bar{p}+1+\hat{m},\bar{k}+\hat{m})}\phi_{\hat{m}}' + F_{(\bar{k}+\hat{m})} = J_{(\bar{k}+\hat{m},1)}\ddot{u}_0 + J_{(\bar{k}+\hat{m},3)}\ddot{\theta}_0 + J_{(\bar{k}+\hat{m},\bar{n}+4)}\ddot{\theta}_{\bar{m}}$$
$$+ \sum_{j=\bar{m}+1}^{\hat{m}-1} J_{(\bar{k}+\hat{m},\bar{k}+j)}\ddot{\theta}_j + J_{(\bar{k}+\hat{m},\bar{k}+\hat{m})}\ddot{\theta}_{\hat{m}} + \sum_{i=\hat{m}+1}^{-1} J_{(\bar{k}+\hat{m},\bar{k}+i)}\ddot{\theta}_i. \tag{54}$$

In a similar way, the charge equations of electrostatics are obtained by collecting the terms related to the variations $\delta\phi_n$ ($n = 1, ..., \bar{n}$) and $\delta\phi_m$ ($m = -1, ..., \bar{m}$), giving

$\delta\phi_n$:

$$P_{(n,1)}u_0' + P_{(n,3)}\theta_0' + \sum_{i=1}^{n-1} P_{(n,i+3)}\theta_i' + P_{(n,n+3)}\theta_n' + C_{(n,n)}\phi_n = \tau_{(n)}, \tag{55}$$

$\delta\phi_m$:

$$P_{(\bar{p}+1+m,1)}u_0' + P_{(\bar{p}+1+m,3)}\theta_0' + P_{(\bar{p}+1+m,\bar{k}+m)}\theta_m' + \sum_{i=m+1}^{-1} P_{(\bar{p}+1+m,\bar{k}+i)}\theta_i' + C_{(\bar{p}+1+m,\bar{p}+1+m)}\phi_m = \tau_{(\bar{p}+1+m)}. \quad (56)$$

The electromechanical boundary conditions at $x = 0, L$ are derived from the applied mechanical forces and electric potentials, and they are defined as

$$\delta u_0\Big(Y_{(1,1)}u_0' + Y_{(1,3)}\theta_0' + \sum_{\hat{n}=1}^{\bar{n}-1} Y_{(1,\hat{n}+3)}\theta_{\hat{n}}' + Y_{(1,\bar{n}+3)}\theta_{\bar{n}}' + Y_{(1,\bar{n}+4)}\theta_{\bar{m}}' + \sum_{\hat{m}=\bar{m}+1}^{-1} Y_{(1,\bar{k}+\hat{m})}\theta_{\hat{m}}' + \sum_{n=1}^{\bar{n}} P_{(n,1)}\phi_n + \sum_{m=\bar{m}}^{-1} P_{(\bar{p}+1+m,1)}\phi_m\Big) = 0, \quad (57)$$

$$\delta w_0\Big(G_{(2,2)}w_0' + G_{(2,3)}\theta_0 + \sum_{\hat{n}=1}^{\bar{n}-1} G_{(2,\hat{n}+3)}\theta_{\hat{n}} + G_{(2,\bar{n}+3)}\theta_{\bar{n}} + G_{(2,\bar{n}+4)}\theta_{\bar{m}} + \sum_{\hat{m}=\bar{m}+1}^{-1} G_{(2,\bar{k}+\hat{m})}\theta_{\hat{m}}\Big) = 0, \quad (58)$$

$$\delta\theta_0\Big(Y_{(3,1)}u_0' + Y_{(3,3)}\theta_0' + \sum_{\hat{n}=1}^{\bar{n}-1} Y_{(3,\hat{n}+3)}\theta_{\hat{n}}' + Y_{(3,\bar{n}+3)}\theta_{\bar{n}}' + Y_{(3,\bar{n}+4)}\theta_{\bar{m}}' + \sum_{\hat{m}=\bar{m}+1}^{-1} Y_{(3,\bar{k}+\hat{m})}\theta_{\hat{m}}' + \sum_{n=1}^{\bar{n}} P_{(n,3)}\phi_n + \sum_{m=\bar{m}}^{-1} P_{(\bar{p}+1+m,3)}\phi_m\Big) = 0, \quad (59)$$

$$\delta\theta_{\hat{n}}\Big(Y_{(\hat{n}+3,1)}u_0' + Y_{(\hat{n}+3,3)}\theta_0' + \sum_{i=1}^{\hat{n}-1} Y_{(\hat{n}+3,i+3)}\theta_i' + Y_{(\hat{n}+3,\hat{n}+3)}\theta_{\hat{n}}' + \sum_{j=\hat{n}+1}^{\bar{n}-1} Y_{(\hat{n}+3,j+3)}\theta_j' + Y_{(\hat{n}+3,\bar{n}+3)}\theta_{\bar{n}}' + P_{(\hat{n},\hat{n}+3)}\phi_{\hat{n}} + \sum_{i=\hat{n}+1}^{\bar{n}} P_{(i,\hat{n}+3)}\phi_i\Big) = 0, \quad (60)$$

$$\delta\theta_{\bar{n}}\Big(Y_{(\bar{n}+3,1)}u_0' + Y_{(\bar{n}+3,3)}\theta_0' + \sum_{\hat{n}=1}^{\bar{n}-1} Y_{(\bar{n}+3,\hat{n}+3)}\theta_{\hat{n}}' + Y_{(\bar{n}+3,\bar{n}+3)}\theta_{\bar{n}}' + P_{(\bar{n},\bar{n}+3)}\phi_{\bar{n}}\Big) = 0, \quad (61)$$

$$\delta\theta_{\bar{m}}\Big(Y_{(\bar{n}+4,1)}u_0' + Y_{(\bar{n}+4,3)}\theta_0' + Y_{(\bar{n}+4,\bar{n}+4)}\theta_{\bar{m}}' + \sum_{\hat{m}=\bar{m}+1}^{-1} Y_{(\bar{n}+4,\bar{k}+\hat{m})}\theta_{\hat{m}}' + P_{(\bar{p}+1+\bar{m},\bar{k}+\bar{m})}\phi_{\bar{m}}\Big) = 0, \quad (62)$$

$$\delta\theta_{\hat{m}}\Big(Y_{(\bar{k}+\hat{m},1)}u_0' + Y_{(\bar{k}+\hat{m},3)}\theta_0' + Y_{(\bar{k}+\hat{m},\bar{n}+4)}\theta_{\bar{m}}' + \sum_{j=\bar{m}+1}^{\hat{m}-1} Y_{(\bar{k}+\hat{m},\bar{k}+j)}\theta_j' + Y_{(\bar{k}+\hat{m},\bar{k}+\hat{m})}\theta_{\hat{m}}' + \sum_{i=\hat{m}+1}^{-1} Y_{(\bar{k}+\hat{m},\bar{k}+i)}\theta_i' + P_{(\bar{p}+1+\hat{m},\bar{k}+\hat{m})}\phi_{\hat{m}} + \sum_{i=\bar{m}}^{\hat{m}-1} P_{\left(\bar{p}+1+i,\bar{k}+\hat{m}\right)}\phi_i\Big) = 0. \quad (63)$$

The symmetric inertial terms $J_{(i,j)} = J_{(j,i)}$, extensional stiffness terms $Y_{(i,j)} = Y_{(j,i)}$, shear stiffness terms $G_{(i,j)} = G_{(j,i)}$, piezoelectric equivalent stiffness terms $P_{(l,i)}$ and capacitance terms $C_{(l,l)}$ ($i, j = 1, \ldots, \bar{k} - 1$ and $l = 1, \ldots, \bar{p}$) in Equations (48)-(63), are given by

$$J_{(1,1)} = \sum_{k=\bar{m}}^{\bar{n}} \rho_k A_k,\ J_{(1,3)} = \sum_{n=1}^{\bar{n}} \rho_n h_0 A_n - \sum_{m=\bar{m}}^{-1} \rho_m h_0 A_m,\ J_{(1,\hat{n}+3)} = \sum_{i=\hat{n}+1}^{\bar{n}} \rho_i 2h_{\hat{n}} A_i$$

$$+\rho_{\hat{n}} \bar{I}_{\hat{n}},\ J_{(1,\bar{n}+3)} = \rho_{\bar{n}} \bar{I}_{\bar{n}},\ J_{(1,\bar{n}+4)} = \rho_{\bar{m}} \bar{I}_{\bar{m}},\ J_{(1,\bar{k}+\hat{m})} = -\sum_{i=\bar{m}}^{\hat{m}-1} \rho_i 2h_{\hat{m}} A_i + \rho_{\hat{m}} \bar{I}_{\hat{m}},$$

$$J_{(2,2)} = \sum_{k=\bar{m}}^{\bar{n}} \rho_k A_k,\ J_{(3,3)} = \sum_{n=1}^{\bar{n}} \rho_n {h_0}^2 A_n + \sum_{m=\bar{m}}^{-1} \rho_m {h_0}^2 A_m + \rho_0 I_0,$$

$$J_{(3,\hat{n}+3)} = 2h_0 h_{\hat{n}} \sum_{i=\hat{n}+1}^{\bar{n}} \rho_i A_i + \rho_{\hat{n}} h_0 \bar{I}_{\hat{n}},\ J_{(3,\bar{n}+3)} = \rho_{\bar{n}} h_0 \bar{I}_{\bar{n}},\ J_{(3,\bar{n}+4)} = -\rho_{\bar{m}} h_0 \bar{I}_{\bar{m}},$$

$$J_{(3,\bar{k}+\hat{m})} = 2h_0 h_{\hat{m}} \sum_{i=\bar{m}}^{\hat{m}-1} \rho_i A_i - \rho_{\hat{m}} h_0 \bar{I}_{\hat{m}},\ J_{(\hat{n}+3,\hat{n}+3)} = \sum_{i=\hat{n}+1}^{\bar{n}} \rho_i 4{h_{\hat{n}}}^2 A_i + \rho_{\hat{n}} I_{\hat{n}},$$

$$J_{(\hat{n}+3,j+3)} = \sum_{i=j+1}^{\bar{n}} \rho_i 4h_{\hat{n}} h_j A_i + \rho_j 2h_{\hat{n}} \bar{I}_j,\ J_{(\hat{n}+3,\bar{n}+3)} = \rho_{\bar{n}} 2h_{\hat{n}} \bar{I}_{\bar{n}},\ J_{(\bar{n}+3,\bar{n}+3)} = \rho_{\bar{n}} I_{\bar{n}},$$

$$J_{(\bar{n}+4,\bar{n}+4)} = \rho_{\bar{m}} I_{\bar{m}},\ J_{(\bar{n}+4,\bar{k}+\hat{m})} = -\rho_{\bar{m}} 2h_{\hat{m}} \bar{I}_{\bar{m}},\ J_{(\bar{k}+\hat{m},\bar{k}+\hat{m})} = \sum_{i=\bar{m}}^{\hat{m}-1} \rho_i 4{h_{\hat{m}}}^2 A_i + \rho_{\hat{m}} I_{\hat{m}},$$

$$J_{(\bar{k}+\hat{m},\bar{k}+i)} = \sum_{j=\bar{m}}^{\hat{m}-1} \rho_j 4h_{\hat{m}} h_i A_j - \rho_{\hat{m}} 2h_i \bar{I}_{\hat{m}}, \tag{64}$$

$$Y_{(1,1)} = \sum_{k=\bar{m}}^{\bar{n}} c_{11}^{*k} A_k,\ Y_{(1,3)} = \sum_{n=1}^{\bar{n}} c_{11}^{*n} h_0 A_n - \sum_{m=\bar{m}}^{-1} c_{11}^{*m} h_0 A_m,\ Y_{(1,\hat{n}+3)} = \sum_{i=\hat{n}+1}^{\bar{n}} c_{11}^{*i} 2h_{\hat{n}} A_i$$

$$+c_{11}^{*\hat{n}} \bar{I}_{\hat{n}},\ Y_{(1,\bar{n}+3)} = c_{11}^{*\bar{n}} \bar{I}_{\bar{n}},\ Y_{(1,\bar{n}+4)} = c_{11}^{*\bar{m}} \bar{I}_{\bar{m}},\ Y_{(1,\bar{k}+\hat{m})} = -\sum_{i=\bar{m}}^{\hat{m}-1} c_{11}^{*i} 2h_{\hat{m}} A_i + c_{11}^{*\hat{m}} \bar{I}_{\hat{m}},$$

$$Y_{(3,3)} = \sum_{n=1}^{\bar{n}} c_{11}^{*n} {h_0}^2 A_n + \sum_{m=\bar{m}}^{-1} c_{11}^{*m} {h_0}^2 A_m + c_{11}^{*0} I_0,\ Y_{(3,\hat{n}+3)} = 2h_0 h_{\hat{n}} \sum_{i=\hat{n}+1}^{\bar{n}} c_{11}^{*i} A_i$$

$$+c_{11}^{*\hat{n}} h_0 \bar{I}_{\hat{n}},\ Y_{(3,\bar{n}+3)} = c_{11}^{*\bar{n}} h_0 \bar{I}_{\bar{n}},\ Y_{(3,\bar{n}+4)} = -c_{11}^{*\bar{m}} h_0 \bar{I}_{\bar{m}},\ Y_{(3,\bar{k}+\hat{m})} = 2h_0 h_{\hat{m}} \sum_{i=\bar{m}}^{\hat{m}-1} c_{11}^{*i} A_i$$

$$-c_{11}^{*\hat{m}} h_0 \bar{I}_{\hat{m}},\ Y_{(\hat{n}+3,\hat{n}+3)} = \sum_{i=\hat{n}+1}^{\bar{n}} c_{11}^{*i} 4{h_{\hat{n}}}^2 A_i + \bar{c}_{11}^{\hat{n}(\phi)} I_{\hat{n}},\ Y_{(\hat{n}+3,j+3)} = \sum_{i=j+1}^{\bar{n}} c_{11}^{*i} 4h_{\hat{n}} h_j A_i$$

$$+c_{11}^{*j} 2h_{\hat{n}} \bar{I}_j,\ Y_{(\hat{n}+3,\bar{n}+3)} = c_{11}^{*\bar{n}} 2h_{\hat{n}} \bar{I}_{\bar{n}},\ Y_{(\bar{n}+3,\bar{n}+3)} = \bar{c}_{11}^{\bar{n}(\phi)} I_{\bar{n}},\ Y_{(\bar{n}+4,\bar{n}+4)} = \bar{c}_{11}^{\bar{m}(\phi)} I_{\bar{m}},$$

$$Y_{(\bar{n}+4,\bar{k}+\hat{m})} = -c_{11}^{*\bar{m}} 2h_{\hat{m}} \bar{I}_{\bar{m}},\ Y_{\left(\bar{k}+\hat{m},\bar{k}+\hat{m}\right)} = \sum_{i=\bar{m}}^{\hat{m}-1} c_{11}^{*i} 4{h_{\hat{m}}}^2 A_i + \bar{c}_{11}^{\hat{m}(\phi)} I_{\hat{m}},$$

$$Y_{\left(\bar{k}+\hat{m},\bar{k}+i\right)} = \sum_{j=\bar{m}}^{\hat{m}-1} c_{11}^{*j} 4h_{\hat{m}} h_i A_j - c_{11}^{*\hat{m}} 2h_i \bar{I}_{\hat{m}}, \tag{65}$$

$$G_{(2,2)} = \sum_{n=1}^{\bar{n}} \bar{c}_{55}^{n(\phi)} A_n + c_{55}^0 A_0 + \sum_{m=\bar{m}}^{-1} \bar{c}_{55}^{m(\phi)} A_m,\ G_{(2,3)} = -c_{55}^0 A_0,\ G_{(2,\hat{n}+3)} = -\bar{c}_{55}^{\hat{n}(\phi)} A_{\hat{n}},$$
$$G_{(2,\bar{n}+3)} = -\bar{c}_{55}^{\bar{n}(\phi)} A_{\bar{n}},\ G_{(2,\bar{n}+4)} = -\bar{c}_{55}^{\bar{m}(\phi)} A_{\bar{m}},\ G_{(2,\bar{k}+\hat{m})} = -\bar{c}_{55}^{\hat{m}(\phi)} A_{\hat{m}},\ G_{(3,3)} = c_{55}^0 A_0,$$
$$G_{(\hat{n}+3,\hat{n}+3)} = \bar{c}_{55}^{\hat{n}(\phi)} A_{\hat{n}},\ G_{(\bar{n}+3,\bar{n}+3)} = \bar{c}_{55}^{\bar{n}(\phi)} A_{\bar{n}},\ G_{(\bar{n}+4,\bar{n}+4)} = \bar{c}_{55}^{\bar{m}(\phi)} A_{\bar{m}},$$
$$G_{\left(\bar{k}+\hat{m},\bar{k}+\hat{m}\right)} = \bar{c}_{55}^{\hat{m}(\phi)} A_{\hat{m}}, \tag{66}$$

$$P_{(n,1)} = \frac{e_{31}^{*n}}{2h_n} A_n,\ P_{(n,3)} = \frac{e_{31}^{*n}}{2h_n} h_0 A_n,\ P_{(n,i+3)} = \frac{e_{31}^{*n}}{2h_n} 2h_i A_n,\ P_{(n,n+3)} = \frac{e_{31}^{*n}}{2h_n} \bar{I}_n,$$
$$P_{(\bar{p}+1+m,1)} = \frac{e_{31}^{*m}}{2h_m} A_m,\ P_{(\bar{p}+1+m,3)} = -\frac{e_{31}^{*m}}{2h_m} h_0 A_m,\ P_{\left(\bar{p}+1+m,\bar{k}+m\right)} = \frac{e_{31}^{*m}}{2h_m} \bar{I}_m,$$
$$P_{\left(\bar{p}+1+m,\bar{k}+i\right)} = -\frac{e_{31}^{*m}}{2h_m} 2h_i A_m, \tag{67}$$

$$C_{(n,n)} = -\frac{\varepsilon_{33}^{*n} A_n}{4{h_n}^2},\ C_{(\bar{p}+1+m,\bar{p}+1+m)} = -\frac{\varepsilon_{33}^{*m} A_m}{4{h_m}^2}. \tag{68}$$

Finally, the applied mechanical forces $F_{(i)}$ and electric charge densities $\tau_{(l)}$ terms are defined as

$$F_{(1)} = \sum_{k=\bar{m}}^{\bar{n}} X_k,\ F_{(2)} = \sum_{k=\bar{m}}^{\bar{n}} Z_k,\ F_{(3)} = \sum_{n=1}^{\bar{n}} h_0 X_n + M_0 - \sum_{m=\bar{m}}^{-1} h_0 X_m,$$
$$F_{(\hat{n}+3)} = h_{\hat{n}} X_{\hat{n}} + \sum_{i=\hat{n}+1}^{\bar{n}} 2h_{\hat{n}} X_i + M_{\hat{n}},\ F_{(\bar{n}+3)} = h_{\bar{n}} X_{\bar{n}} + M_{\bar{n}},$$
$$F_{(\bar{n}+4)} = -h_{\bar{m}} X_{\bar{m}} + M_{\bar{m}},\ F_{\left(\bar{k}+\hat{m}\right)} = -h_{\hat{m}} X_{\hat{m}} - \sum_{i=\bar{m}}^{\hat{m}-1} 2h_{\hat{m}} X_i + M_{\hat{m}}, \tag{69}$$

$$\tau_{(n)} = -b\tau_n, \tau_{(\bar{p}+1+m)} = -b\tau_m. \tag{70}$$

Equations (48)-(63) represent the analytical electro-mechanical model of the layered beam with arbitrary ACLD treatments where the electric potential differences and the generalized mechanical displacements are the unknown independent variables.

3 Finite Element Model

In this section a FE model based on the weak forms of Equations (48)-(56), governing the motion and electric charge equilibrium of the layered beam with piezoelectric and viscoelastic layers, is developed. For convenience, the generalized mechanical displacements and electric potential differences are grouped in the generalized vectors of displacement and potential difference,

$$\mathbf{u}(x,t) = \{u_0(x,t), w_0(x,t), \theta_0(x,t), \theta_1(x,t), \ldots, \theta_{\bar{n}}(x,t), \theta_{\bar{m}}(x,t), \ldots, \theta_{-1}(x,t)\}^{\mathrm{T}}, \tag{71}$$

$$\boldsymbol{\phi}(x,t) = \left\{\phi_1(x,t), \ldots, \phi_{\bar{n}}(x,t), \phi_{\bar{m}}(x,t), \ldots, \phi_{-1}(x,t)\right\}^{\mathrm{T}}. \tag{72}$$

The weak forms are given by

$$\int_L \left[\delta\mathbf{u}^{\mathrm{T}}\mathbf{J}\ddot{\mathbf{u}} + \delta\mathbf{u}^{\mathrm{T}}(\mathbf{L}_{xx}^{\mathrm{T}}\mathbf{Y}\mathbf{L}_{xx} + \mathbf{L}_{xz}^{\mathrm{T}}\mathbf{G}\mathbf{L}_{xz})\mathbf{u} + \delta\mathbf{u}^{\mathrm{T}}\mathbf{L}_{xx}^{\mathrm{T}}\mathbf{P}^{\mathrm{T}}\boldsymbol{\phi}\right] \mathrm{d}L = \int_L \delta\mathbf{u}^{\mathrm{T}}\mathbf{F}\ \mathrm{d}L, \tag{73}$$

$$\int_L (\delta\boldsymbol{\phi}^{\mathrm{T}}\mathbf{P}\mathbf{L}_{xx}\mathbf{u} + \delta\boldsymbol{\phi}^{\mathrm{T}}\mathbf{C}\boldsymbol{\phi})\mathrm{d}L = \int_L \delta\boldsymbol{\phi}^{\mathrm{T}}\boldsymbol{\tau}\ \mathrm{d}L. \tag{74}$$

The non-zero terms of the symmetric positive definite inertia matrix $\mathbf{J}$ and of the symmetric semi-positive definite extensional and shear stiffness matrices $\mathbf{Y}$ and $\mathbf{G}$, of size $[(\bar{k}-1)\times(\bar{k}-1)]$, are defined in (64), (65) and (66), respectively. The piezoelectric equivalent stiffness and capacitance matrices $\mathbf{P}$ and $\mathbf{C}$, of sizes $[\bar{p}\times(\bar{k}-1)]$ and $(\bar{p}\times\bar{p})$ respectively, have non-zero terms defined by (67) and (68). The applied mechanical forces and electric charge density vectors $\mathbf{F}$ and $\boldsymbol{\tau}$, of size $[(\bar{k}-1)\times 1]$ and $(\bar{p}\times 1)$, respectively, have elements defined by (69) and (70). The differential operators

$$\mathbf{L}_{xx} = diag\left(\frac{\partial}{\partial x}, 0, \frac{\partial}{\partial x}, \cdots, \frac{\partial}{\partial x}\right), \mathbf{L}_{xz} = diag\left(0, \frac{\partial}{\partial x}, 1, \cdots, 1\right). \tag{75}$$

of size $[(\bar{k}-1)\times(\bar{k}-1)]$ are used for the definition of the generalized extensional and shear strains.

With the purpose of obtaining an approximated solution of Equations (73) and (74), the FE method involving a transformation of the global integral forms to a representation composed of the sum of the elemental integral forms is utilized, leading to the definition of the local (elemental) matrices and vectors. Thus, the beam's total length L is divided and the domain of integration is discretized into q finite elements of length L_e, leading to a FE mesh composed of $q+1$ nodal points. With the sum taken over all q elements the global weak forms become

$$\sum_{e=1}^{q}\int_{L_e} \delta\mathbf{u}^{e\mathrm{T}}\left[\mathbf{J}\ddot{\mathbf{u}}^e + \left(\mathbf{L}_{xx}^{\mathrm{T}}\mathbf{Y}\mathbf{L}_{xx} + \mathbf{L}_{xz}^{\mathrm{T}}\mathbf{G}\mathbf{L}_{xz}\right)\mathbf{u}^e + \mathbf{L}_{xx}^{\mathrm{T}}\mathbf{P}^{\mathrm{T}}\boldsymbol{\phi}^e - \mathbf{F}\right] \mathrm{d}L_e = 0, \tag{76}$$

$$\sum_{e=1}^{q}\int_{L_e} \delta\boldsymbol{\phi}^{e\mathrm{T}}(\mathbf{P}\mathbf{L}_{xx}\mathbf{u}^e + \mathbf{C}\boldsymbol{\phi}^e - \boldsymbol{\tau}^e)\ \mathrm{d}L_e = 0. \tag{77}$$

The mechanical (and its second time derivative) and electrical variables $\mathbf{u}^e(x,t)$ and $\boldsymbol{\phi}^e(x,t)$ of (76) and (77) are restricted to the domain of integration and the approximation is considered at a local level in each sub-domain. Furthermore, only the nodal values of the variables at the element boundaries contribute to the approximation.

For the definition of the local approximation of the generalized mechanical and electrical DoFs in each sub-domain, a generic element with two nodes (1 and 2) is isolated from the FE mesh (Figure 2). The correspondence between each node of the element and the global node enumeration is established through the mechanical $\mathbf{R}_u^e$ and electrical $\mathbf{R}_\phi^e$ connectivity matrices,

$$\bar{\mathbf{u}}^e = \mathbf{R}_u^e\bar{\mathbf{u}},\ \bar{\boldsymbol{\phi}}^e = \mathbf{R}_\phi^e\bar{\boldsymbol{\phi}}, \tag{78a,b}$$

with the mechanical $\bar{\mathbf{u}}^e$ and electrical $\bar{\boldsymbol{\phi}}^e$ elemental DoF vectors defined as

$$\bar{\mathbf{u}}^e = \left\{\bar{u}_0^1, \bar{w}_0^1, \bar{\theta}_0^1, \bar{\theta}_1^1, \cdots, \bar{\theta}_{\bar{n}}^1, \bar{\theta}_{\bar{m}}^1, \cdots, \bar{\theta}_{-1}^1, \bar{u}_0^2, \bar{w}_0^2, \bar{\theta}_0^2, \bar{\theta}_1^2, \cdots, \bar{\theta}_{\bar{n}}^2, \bar{\theta}_{\bar{m}}^2, \cdots, \bar{\theta}_{-1}^2\right\}^{\mathrm{T}}, \tag{79}$$

$$\bar{\boldsymbol{\phi}}^e = \left\{\bar{\phi}_1, \cdots, \bar{\phi}_{\bar{n}}, \bar{\phi}_{\bar{m}}, \cdots, \bar{\phi}_{-1}\right\}^{\mathrm{T}}. \tag{80}$$

The connectivity matrices are of size $[\bar{k}(q+1)\times\bar{k}(q+1)]$ and $(\bar{p}q \times \bar{p}q)$, respectively, and the superscript 1 or 2 denotes the node at which the DoF is defined, while the subscript identifies the layer to which the DoF refers. As usual, a variable from the global DoF mechanical vector appears on two DoF elemental vectors, except for the boundary nodes of the global domain. However, for the electrical case this is not the case because continuity of the electric potential difference between adjacent FEs is not assured.

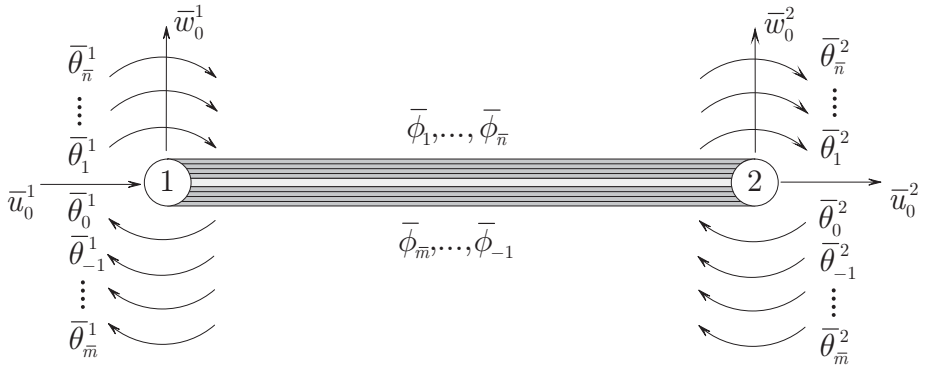

Figure 2: One-dimensional FE of the beam with arbitrary ACLD treatments.

From the differential operators (75) it is possible to see that the variational Equations (73) and (74) contain at most first order derivatives of the generalized displacements and zero order derivatives of the electric potential differences. Thus, the displacement variables within each element domain must be, at least, approximated by linear interpolation functions. For the electric potential differences, constant functions are utilized and the electric potential difference becomes constant in each element. The interpolation functions are grouped in the mechanical and electrical interpolation matrices $\mathbf{N}_u$ and $\mathbf{N}_\phi$. Therefore, the generalized displacement and electric potential vectors in each sub-domain are approximated by

$$\mathbf{u}^e(x,t) = \mathbf{N}_u \bar{\mathbf{u}}^e, \;\; \boldsymbol{\phi}^e(x,t) = \mathbf{N}_\phi \bar{\boldsymbol{\phi}}^e. \tag{81a,b}$$

Considering the relations in (81), the Equations (76) and (77) can be written as

$$\sum_{e=1}^{q} \delta\bar{\mathbf{u}}^{e\mathrm{T}} \left(\mathbf{M}_{uu}^e \ddot{\bar{\mathbf{u}}}^e + \mathbf{K}_{uu}^e \bar{\mathbf{u}}^e + \mathbf{K}_{u\phi}^e \bar{\boldsymbol{\phi}}^e - \mathbf{F}^e\right) = 0, \tag{82}$$

$$\sum_{e=1}^{q} \delta\bar{\boldsymbol{\phi}}^{e\mathrm{T}} \left(\mathbf{K}_{\phi u}^e \bar{\mathbf{u}}^e + \mathbf{K}_{\phi\phi}^e \bar{\boldsymbol{\phi}}^e - \mathbf{Q}^e\right) = 0, \tag{83}$$

where the elemental matrices and vectors are defined as

$$\mathbf{M}_{uu}^{e} = \int_{L_e} \mathbf{N}_u^{\mathrm{T}} \mathbf{J} \mathbf{N}_u \, \mathrm{d}L_e, \;\; \mathbf{K}_{uu}^{e} = \int_{L_e} (\mathbf{B}_{xx}^{\mathrm{T}} \mathbf{Y} \mathbf{B}_{xx} + k_s \mathbf{B}_{xz}^{\mathrm{T}} \mathbf{G} \mathbf{B}_{xz}) \, \mathrm{d}L_e, \tag{84a,b}$$

$$\mathbf{K}_{u\phi}^{e} = \mathbf{K}_{\phi u}^{e\mathrm{T}} = \int_{L_e} \mathbf{B}_{xx}^{\mathrm{T}} \mathbf{P}^{\mathrm{T}} \, \mathrm{d}L_e, \;\; \mathbf{K}_{\phi\phi}^{e} = \int_{L_e} \mathbf{N}_{\phi}^{\mathrm{T}} \mathbf{C} \mathbf{N}_{\phi} \, \mathrm{d}L_e, \tag{85a,b}$$

$$\mathbf{F}^{e} = \int_{L_e} \mathbf{N}_u^{\mathrm{T}} \mathbf{F} \, \mathrm{d}L_e, \;\; \mathbf{Q}^{e} = \int_{L_e} \mathbf{N}_{\phi}^{\mathrm{T}} \boldsymbol{\tau} \, \mathrm{d}L_e, \tag{86a,b}$$

and the extensional and shear deformation matrices utilized are given by

$$\mathbf{B}_{xx} = \mathbf{L}_{xx} \mathbf{N}_u, \mathbf{B}_{xz} = \mathbf{L}_{xz} \mathbf{N}_u. \tag{87a,b}$$

A shear correction factor k_s is introduced in order to approximate the effects of the non-linear shear deformation distribution [13]. Furthermore, reduced integration of the higher order terms of the shear stiffness matrix should be used in order to overcome the overstiffening of the element at low thickness (shear locking).

Considering relations (78) and substituting them into (82) and (83), the global equations of motion and electric charge equilibrium of the discrete system take the form

$$\forall \delta \bar{\mathbf{u}} : \quad \mathbf{M}_{uu} \ddot{\bar{\mathbf{u}}} + \mathbf{K}_{uu} \bar{\mathbf{u}} + \mathbf{K}_{u\phi} \bar{\boldsymbol{\phi}} = \mathbf{F}, \tag{88}$$

$$\forall \delta \bar{\boldsymbol{\phi}} : \quad \mathbf{K}_{\phi u} \bar{\mathbf{u}} + \mathbf{K}_{\phi\phi} \bar{\boldsymbol{\phi}} = \mathbf{Q}, \tag{89}$$

with the global matrices and vectors defined by

$$\mathbf{M}_{uu} = \sum_{e=1}^{q} \mathbf{R}_u^{e\mathrm{T}} \mathbf{M}_{uu}^{e} \mathbf{R}_u^{e}, \;\; \mathbf{K}_{uu} = \sum_{e=1}^{q} \mathbf{R}_u^{e\mathrm{T}} \mathbf{K}_{uu}^{e} \mathbf{R}_u^{e}, \tag{90a,b}$$

$$\mathbf{K}_{u\phi} = \mathbf{K}_{\phi u}^{\mathrm{T}} = \sum_{e=1}^{q} \mathbf{R}_u^{e\mathrm{T}} \mathbf{K}_{u\phi}^{e} \mathbf{R}_{\phi}^{e}, \mathbf{K}_{\phi\phi} = \sum_{e=1}^{q} \mathbf{R}_{\phi}^{e\mathrm{T}} \mathbf{K}_{\phi\phi}^{e} \mathbf{R}_{\phi}^{e}, \tag{91a,b}$$

$$\mathbf{F} = \sum_{e=1}^{q} \mathbf{R}_u^{e\mathrm{T}} \mathbf{F}^{e}, \mathbf{Q} = \sum_{e=1}^{q} \mathbf{R}_{\phi}^{e\mathrm{T}} \mathbf{Q}^{e}. \tag{92a,b}$$

The FE model of the beam with arbitrary ACLD treatments is described by the elemental matrices and vectors in Equations (84)-(86) and by the global FE equations of motion and charge equilibrium in Equations (88)-(89).

4 Experimental Validation

In order to validate the presented FE model some measurements were taken on an aluminium beam with a partial ACLD treatment (viscoelastic layer sandwiched between the piezoelectric patch and the base beam). The analysis concerned free-free boundary conditions. The beam was 400 mm long, 2.92 mm thick and 30 mm wide, and the ACLD treatment was 50 mm long and 30 mm wide, with viscoelastic and piezoelectric

layers of thickness 0.127 mm and 0.5 mm, respectively. Taking one end of the beam to be $x = 0$, the ACLD treatment was positioned slightly off-center on the beam, starting at $x = 202$ mm, and was realized with a passive viscoelastic layer of a material manufactured by 3M (ISD112) and a piezoelectric constraining patch manufactured by PI (PIC 255). The shear storage modulus and loss factor of the viscoelastic material at the experiment temperature ($22\ ^o$C) were extracted from the manufacturer's nomogram [14]. The mechanical and electrical material properties of the aluminium beam, viscoelastic layer and piezoelectric patch, are presented in Table 1.

Aluminium		3M ISD112	PIC 255			
c_{11}^*	69 GPa	—	c_{11}^*	62.11 GPa	e_{31}^*	-11.18 C/m^2
c_{55}	26.54 GPa	—	c_{55}	23.89 GPa	e_{15}	11.94 C/m^2
ρ	2700 Kg/m^3	1130 Kg/m^3	ρ	7800 Kg/m^3	ε_{11}	12.6×10^{-9} F/m
					ε_{33}^*	9.96×10^{-9} F/m

Table 1: Properties of the aluminium, viscoelastic layer and piezoelectric patch.

The FE model implementation was realized in MATLAB® and an hysteretic damping model with a loss factor equal to 2×10^{-3} was considered in the numerical evaluations. Three frequency response functions were measured experimentally and evaluated numerically: acceleration per unit force (accelerance), acceleration per unit voltage into the piezoelectric patch and induced voltage per unit force. The excitation and response locations were at $x = 275$ mm. The results are shown in Figures 3 to 5.

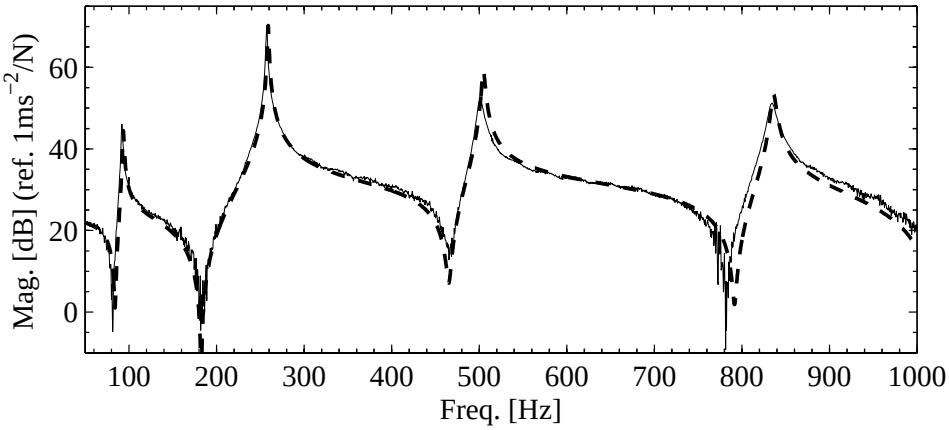

Figure 3: Frequency response function (acceleration per unit force) of the beam with ACLD treatment: _ _ _ , numerical; _____ , experimental.

As can be seen, there is very good agreement between the numerical and experimental results. Both the dynamics of the system and the actuating and sensing capabilities of the piezoelectric patch are validated.

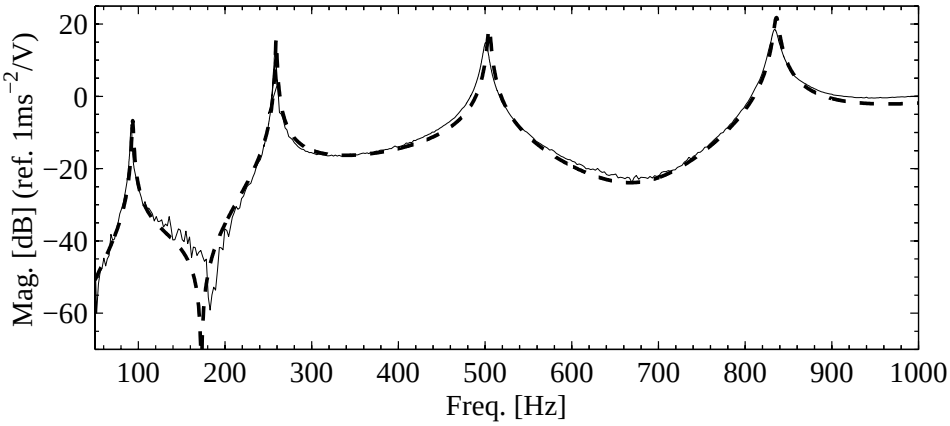

Figure 4: Frequency response function (acceleration per unit voltage) of the beam with ACLD treatment: _ _ _ , numerical; _____ , experimental.

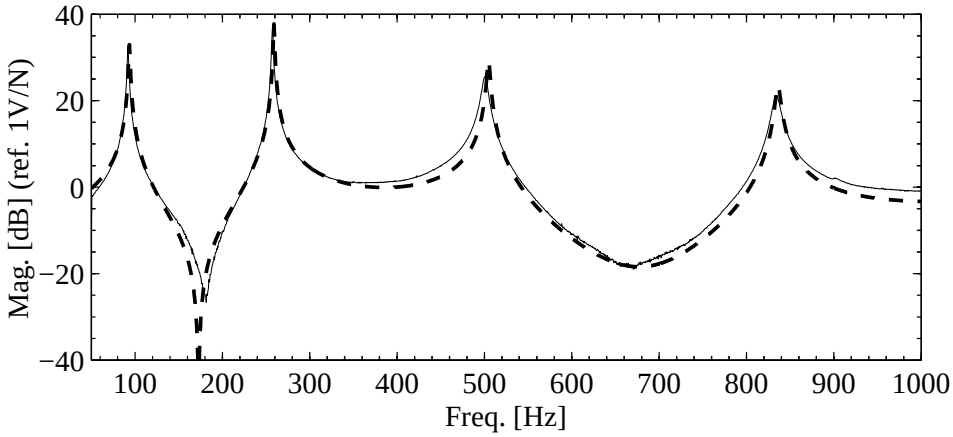

Figure 5: Frequency response function (voltage per unit force) of the beam with ACLD treatment: _ _ _ , numerical; _____ , experimental.

5 Conclusion

In this paper a generic analytical formulation and FE solution for the study of arbitrary ACLD treatments in beams was presented. The ability of the method to accurately model the hybrid behavior, elastic, viscoelastic and piezoelectric materials, was validated against experimental results. The analytical formulation can be used for other solution methods and the FE model can be used in the simulation of active control systems in beams with arbitrary ACLD treatments.

References

[1] A. Benjeddou. *"Advances in hybrid active-passive vibration and noise control via piezoelectric and viscoelastic constrained layer treatments"*. Journal of Vi-

bration and Control, 7(4):565–602, 2001.

[2] C. H. Park and A. Baz. *"Vibration damping and control using active constrained layer damping: A survey"*. The Shock and Vibration Digest, 31(5):355–364, 1999.

[3] R. A. Moreira and J. D. Rodrigues. *"The modelisation of constrained damping layer treatment using the finite element method: Spatial and viscoelastic behavior"*. In International Conference on Structural Dynamics Modelling: Test, Analysis Correlation and Validation, Madeira, PT, 2002.

[4] D. J. McTavish and P. C. Hughes. *"Modeling of linear viscoelastic space structures"*. Journal of Vibration and Acoustics, 115(1):103–110, 1993.

[5] G. A. Lesieutre and E. Bianchini. *"Time domain modeling of linear viscoelasticity using anelastic displacement fields"*. Journal of Vibration and Acoustics, 117(4):424–430, 1995.

[6] R. L. Bagley and P. J. Torvik. *"Fractional calculus in the transient analysis of viscoelastically damped structures"*. AIAA Journal, 23(6):918–925, 1985.

[7] A. Benjeddou. *"Advances in piezoelectric finite element modelling of adaptive structural elements: A survey"*. Computers and Structures, 76(1-3):347–363, 2000.

[8] C. M. A. Vasques, B. Mace, P. Gardonio and J. D. Rodrigues. *"Analytical formulation and finite element modelling of beams with arbitrary active constrained layer damping treatments"*. Institute of Sound and Vibration Research, Technical Memorandum TM934, Southampton, UK, 2004.

[9] J. F. Nye. *"Physical properties of crystals: Their representation by tensors and matrices"*. Clarendon Press, Oxford, UK, 1957.

[10] M. Krommer and H. Irschik. *"On the influence of the electric field on free transverse vibrations of smart beams"*. Smart Materials and Structures, 8(3):401–410, 1999.

[11] C. M. A. Vasques and J. D. Rodrigues. *"Coupled three-layered analysis of smart piezoelectric beams with different electric boundary conditions"*. International Journal for Numerical Methods in Engineering, in revision.

[12] H. F. Tiersten. *"Linear piezoelectric plate vibrations"*. Plenum Press, New York, USA, 1969.

[13] V. Birman and C. W. Bert. *"On the choice of shear correction factor in sandwich structures"*. Journal of Sandwich Structures and Materials, 4:83–95, 2002.

[14] 3M. *"Scotchdamp vibration control systems: Product information and performance data"*. 3M Industrial Tape and Specialties Division, St.Paul, USA, 1993.